Materials Chemistry and Physics 239 (2020) 122268

Contents lists available at ScienceDirect

Materials Chemistry and Physics

journal homepage: www.elsevier.com/locate/matchemphys

Meta-halloysite to improve compactness in iron-rich laterite-based alkali activated materials

Cyriaque Rodrigue Kaze [a,*], Paul Venyite [b], Achile Nana [c], Deutou Nemaleu Juvenal [b], Herve Kouamo Tchakoute [a], Hubert Rahier [d], Elie Kamseu [b,e,**], Uphie Chinje Melo [a], Cristina Leonelli [e]

[a] Laboratory of Applied Inorganic Chemistry, Faculty of Science, University of Yaoundé I, P.O. Box 812, Yaoundé, Cameroon
[b] Laboratory of Materials, Local Materials Promotion Authority, MINRESI/MIPROMALO, P.O. Box 2396, Yaoundé, Cameroon
[c] Research Unit of Noxious Chemistry and Environmental Engineering, University of Dschang, Faculty of Science, Department of Chemistry, P.O. Box 67, Dschang, Cameroon
[d] Department Materials and Chemistry, Vrije Universiteit Brussel, Pleinlaan 2, 1050, Brussels, Belgium
[e] Department of Engineering "Enzo Ferrari", University of Modena and Reggio Emilia, ViaP. Vicarelli 10, 41125, Modena, Italy

HIGHLIGHTS

- Calcined laterite at 600 °C was used to synthesize geopolymers cured at ambient temperature.
- Incorporation of *meta*-halloysite into geopolymer matrix extended the amorphous phase.
- Compressive strength of laterite-based geopolymer increased with *meta*-halloysite added.
- Adding an optimum of *meta*-halloysite powder inhibited the efflorescence formation.

ARTICLE INFO

Keywords:
Laterite
meta-Halloysite
Geopolymer composite
Shrinkage
Mechanical strength
Efflorescence

ABSTRACT

In this paper, the results of the experimental investigation were used to understand the effect of fine *meta*-halloysite on the reactivity, mechanical and microstructural properties of laterite-based geopolymers. Laterite was replaced by 0, 20, 30 and 50 wt% of *meta*-halloysite in order to improve the physico-chemical performance. *Meta*-halloysite was prepared by calcination of natural halloysite at 600 °C. The moduli (molar ratio SiO_2/Na_2O) of the activating solutions were 1.04, 0.92, and 0.75 with $H_2O/Na_2O = 9.78$, 10.45 and 12.04, respectively. The results indicated that calcined laterite has a high specific surface area ($43.00 \pm 0.12\ m^2/g$), notwithstanding a high average particle size ($d_{50} = 45.20\ \mu m$) compared to *meta*-halloysite with a smaller average particle size ($d_{50} = 8.40\ \mu m$) and a specific surface ($29.80 \pm 0.16\ m^2/g$). The compressive strength of geopolymers increased upon the addition of *meta*-halloysite from 12 MPa to 45 MPa at 28 days. While the setting time and water absorption decrease with increase in the of *meta*-halloysite content as well as with increase in Si/Al, Si/Fe, Al/Fe and Na/Al molar ratios used in the synthesis of geopolymers. The use of fine *meta*-halloysite resulted in better efficiency and improved mechanical performance of synthesized products.

1. Introduction

The term geopolymer was introduced in 1970s by Joseph Davidovits to describe alkali aluminosilicate binders formed via the addition of aluminosilicate materials (metakaolin, dolomite) to an alkaline solution [1]. In the literature, several investigations have used different types of aluminosilicate materials in the designs of geopolymer composites including metakaolin, fly ash, slag, volcanic scoria etc. [2–5]. These last years, lateritic soils with relatively high amounts of iron oxide were involved in the geopolymer synthesis and the resulting products are not very good (≤20 MPa) [6–10]. Lateritic soils are iron-rich aluminosilicate materials formed in tropical and subtropical regions, with a high content

* Corresponding author.
** Corresponding author. Laboratory of Materials, Local Materials Promotion Authority, MINRESI/MIPROMALO, P.O. Box 2396, Yaoundé, Cameroon.
E-mail addresses: cyriaque.kaze@uy1.uninet.cm, kazerodrigue@gmail.com (C.R. Kaze), kamseuelie2001@yahoo.fr (E. Kamseu).

https://doi.org/10.1016/j.matchemphys.2019.122268
Received 28 May 2019; Received in revised form 3 October 2019; Accepted 7 October 2019
Available online 15 October 2019
0254-0584/

of iron minerals and 10 to 30 wt% of clayey minerals [10]. They represent nearly 67% of tropical territory [11]. However, only a small amount of this material is used in the production of compressed earth blocks stabilized with Portland cement and also as sub-base in earth fill in road constructions by public works enterprises [12]. Further studies on how lateritic soils can be commercialised are thus justified.

The characteristics of the final geopolymer products derived from calcined lateritic soils depend on the calcination temperature, chemical and mineralogical composition of laterite and synthetic conditions. Lecomte et al. [6] stabilized raw lateritic clay with fulvic acid and lime, and obtained 12 MPa of compressive strength. Their synthesis involved acidic and alkaline reactions followed by a curing period of 18 days at 60 °C under water-saturated atmosphere. Kaze et al. [10] studied the effect of temperature of calcination of two iron-rich lateritic soils on the properties of inorganic polymer (geopolymer). They found that the best calcination temperature is lower than 600 °C, because above such temperature there is sintering of particles which reduces dissolution resulting in lower mechanical strength due to the appearance of cracks and voids at level of microstructure. However, the specimens synthesized at room temperature present a white deposit known as efflorescence along their surface, which is due to the reaction between unreacted sodium ions with CO_2 of the atmosphere. Later Kaze et al. [13] investigated the effect of the silica modulus of the activating solution on microstructure and strength development of two calcined iron-rich laterites based geopolymers and, they found that the highest strength is achieved with a silica modulus of 0.75 resulting in a dense and compact structure. In literature, the optimal Si/Al ratio in natural iron-rich laterite is reported to be in the range of 0.1–1.5 [9,10,14–16]. Latifi et al. [17] investigated the strength properties and physicochemical mechanisms related to tropical laterite soil mixed with a commercial liquid soil stabilizer and strengthener. They stated that the strength of the stabilized laterite soil improves significantly due to the new formed cementitious compounds of sodium aluminosilicate hydrate (N–A–S–H). Obonyo et al. [14] carried out a study on the stabilisation of raw iron-rich laterites with 15–35 wt% of a geopolymer based on calcined laterite at 700 °C with low content of iron. They found that flexural strength increases due to the re-establishment of Si/Al, Si/Fe and Al/Fe ratios by the addition of fine calcined laterite (rich in clayey phases). In the same manner, Lemougna et al. [18] added calcite and slag in the improvement of treated indurated laterite at 700 °C and they reported that a possible synergy mix of N-A-S-H network and C-A-S-H gel are responsible for the resulted high strength. Recently, Kaze et al. [19] produced iron-rich aluminosilicate (laterite) composite geopolymers containing 10 to 40 wt% of rice husk ash resulting in the formation of ferri-silicates that changed the flexural strength and microstructure.

Next to the influence on the mechanical properties, the addition of calcined halloysite has an influence on the reaction rate [20]. Zhang et al. [21] studied a kaolin, containing 31 wt % halloysite and compared with a relatively pure kaolin. The results showed that kaolin containing some halloysite heated at 700 °C possessed higher Si and Al dissolution rate than the purer kaolin and its metakaolin. They stated that the presence of halloysite in kaolin led to a higher geopolymerization rate of metakaolin as reflected by the heat evolution rate. Joshi et al. [22] partially replaced fly-ash by 3–6% of natural halloysite clay to improve the setting time of fly-ash particles. They concluded that halloysite does not deliver oxides for the geopolymerization reaction but helps in controlling the solidification time. *Meta*-halloysite was obtained in this study from calcined halloysite at 600 °C. Halloysite mainly consists of alumina and silica with the same theoretical chemical composition as kaolinite, except for its higher water content because unit layers in halloysite are separated by a monolayer of water molecules [23–29]. If we consider the ideal unit formula for kaolinite to be: $Al_2Si_2O_5(OH)_4$, then we have $Al_2Si_2O_5(OH)_4nH_2O$ for halloysite, where for $n = 0$ it is halloysite- (7 Å) and for $n = 2$, halloysite-(10 Å). Halloysite attracted our attention because of the hosting cations, in particular it can show variable Fe^{3+} contents, as observed in kaolinite, in octahedral positions, and this substitution can be greater in halloysite (up to 12.8% of Fe_2O_3) than in kaolinite (up to 7% of Fe_2O_3) [29]. Due to these peculiarities, the addition of *meta*-halloysite in calcined laterite will increase the amount of reactive aluminosilicate phases and improve the chemical and mechanical stabilities of the geopolymers resulting from calcined iron-rich aluminosilicate (laterite) at room temperature.

Hence, a deep understanding of the role of *meta*-halloysite as a secondary source material in laterite-based geopolymer synthesis is necessary. For this reason, in this study the aim is to shorten the setting time and to improve the mechanical properties of samples consisting of calcined laterite at 600 °C by adding 0, 20, 30 and 50 wt% of *meta*-halloysite (MH). To further optimise the material, three activating solutions are used with different Na/Si ratio. The setting time of fresh pastes was assessed using the Vicat needle apparatus. The hardened products were characterized by means of the compressive strength as well as by Fourier Transform Infrared Spectroscopy (FTIR), X-Ray Diffraction (XRD) and Environmental Scanning Electron Microscope (ESEM).

2. Materials and experimental methods

2.1. Materials

The laterite used in this work was extracted from huge quarries at Odza neighbourhood close to Yaoundé town (Centre region in Cameroon), whereas the halloysite clay was collected from Balengou (West region in Cameroon). The calcined laterite at 600 °C, LAT600, was previously studied [30] and is composed of hematite (α-Fe_2O_3, PDF# 33-664), maghemite (γ-Fe_2O_3, PDF# 39-1346, ilmenite ($FeTiO_3$, PDF# 29-733), quartz (SiO_2, PDF# 46-1045), and anatase (TiO_2, PDF# 21-1272) as major mineral phases. *Meta*-halloysite, MH600, (obtained from calcined halloysite clay at 600 °C) contains residual halloyiste ($Al_2Si_2O_5(OH)_4$ PDF# 29-1487), quartz (SiO_2, PDF# 46-1045), ilmenite ($FeTiO_3$, PDF# 29-733), anatase (TiO_2, PDF# 21-1272), and maghemite (γ-Fe_2O_3, PDF# 39-1346). The X-ray diffractograms of starting materials used in this study are presented in Fig. 1. The particle size distribution was determined with a Mastersizer 2000 Ver. 5.22 (Malvern instruments Ltd.) indicating the average particle size d_{50} of 8.40 and 45.20 μm, respectively for calcined halloysite and laterite. The granulometric analysis was performed under ultrasonic condition. The B.E.T. specific surface areas were determined using a method based on nitrogen absorption (GEMINI 2360, Micromeritics) and gave the following mean values: $29.80 \pm 0.16\ m^2/g$ for *meta*-halloysite and $43.00 \pm 0.12\ m^2/g$ for calcined laterite. The clay fraction of halloysite was dried, crushed,

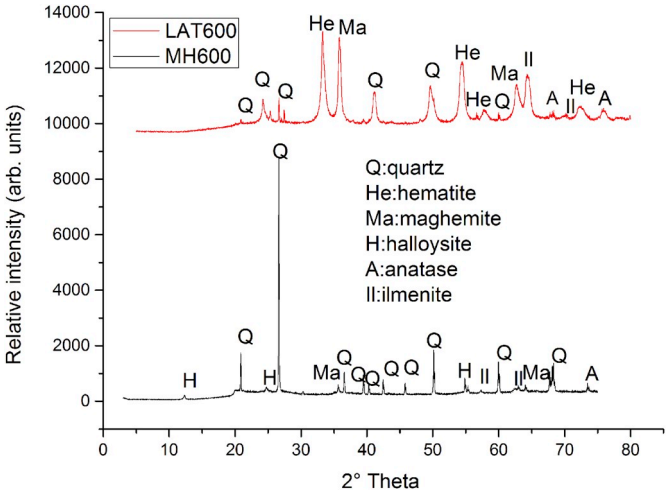

Fig. 1. XRD patterns of calcined laterite (LAT600) and *meta*-halloysite (MH600).

milled and then sieved below 63 μm and calcined at 600 °C for 4 h at a heating rate of 5 °C/min in a programmable electric furnace to increase its reactivity. The chemical compositions of raw materials used as solid precursors was determined using an X-Ray Fluorescence Analysis (Thermo ARL, ARL Advant XP and XP^{+}X-Ray Fluorescence Spectrometer, Thermo Fisher Scientific, MA, USA, Table 1).

2.2. Laterite-meta-halloysite based geopolymer preparation

The geopolymer paste was obtained firstly by mixing the calcined laterite at 600 °C for 5min in a Hobart mixer (M&O model N50-G) with various amounts of fine powder of *meta*-halloysite (0, 20, 30 and 50 wt %). Then, the alkaline solution was added slowly to each geopolymer composite formulation with a liquid/solid ratio of 0.74. The mixture of alkaline solution and solid precursor was mixed for 10 min. The fresh geopolymer pastes obtained were poured into cylindrical molds with dimensions (Ø = 30 mm, h = 60 mm). Once molded, they were vibrated for 5min on an electrical vibrating table to remove entrapped air bubbles. Finally, the samples were sealed into plastic bags to avoid water evaporation and stored at room temperature (25 ± 3 °C) for 24 h before de-molding. The curing continued at room temperature without sealing until 28 days. The geopolymers obtained with 0, 20, 30 and 50 wt% of *meta*-halloysite (MH) blended with calcined laterite are labeled 100/0, 80/20, 70/30 and 50/50 (100, 80, 70 and 50 represent the mass of calcined laterite while 0, 20, 30 and 50 is the mass of *meta*-halloysite). The details of mix design of powders and geopolymer formulations are given in Tables 2 and 3, respectively.

Three alkaline solutions used in this project were obtained by mixing sodium silicate solution (14.37 wt% Na_2O, 29.54 wt% SiO_2, 56.09 wt% H_2O; supplied by Ingessil s.r.l. Verona; Italy. Its density was 1.38 g cm^{-3}) and sodium hydroxide solution (8, 10 and 12 M). The moduli (molar ratio SiO_2/Na_2O) of the activating solutions were 1.04, 0.92, and 0.75 with H_2O/Na_2O = 9.78, 10.45 and 12.04, respectively.

2.3. Characterization methods

The initial and final setting times were measured on the fresh samples using a Vicat apparatus. The test was performed according to the EN 196-3 standard. The needle used was 1.000 ± 0.005 mm in diameter. Measures were repeated three times for each formulation. Then the average values and the standard deviation were calculated. The compressive strength of the samples was measured with an Instron 1195 Compression machine with a displacement of 3 mm/min. The results shown are an average of five replicate specimens. The drying shrinkage was measured with a Vernier Calliper on the hardened laterite-*meta*-halloysite based geopolymers. The length measurement was carried out at the age of 7, 14, 21 or 28 days respectively. Drying shrinkage was calculated according to ASTMC596 using the following equation (1):

$$L = \frac{L_0 - L}{L_0} \times 100 \quad (1)$$

where L_0 is the initial length of specimens at first days and L_7, L_{14}, L_{21} and L_{28} represent the length of specimens measured at 7, 14, 21 and 28 days, respectively.

Table 1
Chemical composition of starting materials.

Oxides (wt %)	Calcined Laterite (LAT600)	*Meta*-halloysite (MH600)
Fe2O3	39.00	2.94
SiO2	28.04	62.0
Al2O3	25.10	32.5
TiO2	0.23	0.37
V2O5	0.14	0.120
P2O5	0.14	0.170
ZrO3	/	1.95
L.O.I	1.95	0.05

Table 2
Chemical design of mixing of laterite-*meta*-halloysite powders.

Geopolymer samples	Si/Al	Si/Fe	Al/Fe
100/0	0.96	0.44	0.46
80/20	1.14	0.73	0.65
70/30	1.22	0.92	0.76
50/50	1.55	1.72	1.11

The water absorption (WA) analysis was carried out by immersing the specimen in water at ambient temperature for 24 h and comparing the humid mass (mh) to the initial dry mass (ms) according to Eq. (2). The water absorption test was carried out according to ASTM C642-06.

$$Wa = \frac{(mh - md)}{md} \; x \; 100 \quad (2)$$

Fourier Transform Infrared Spectroscopy FT-IR, (Avatar 330 FTIR, Thermo Nicolet) was performed on selected samples (analyzing surface and bulk areas). The analysis was done on the pieces collected from the mechanical testing allowing us to have access to the surface and the bulk. A minimum of 32 scans between 4000 and 400 cm^{-1} was averaged for each spectrum at intervals of 1 cm^{-1}.

The geopolymer (100/0, 80/20, 70/30 and 50/50) specimens aged for 28 days were crushed and sieved through a sieve of mesh 80 μm and X-Ray diffractograms were recorded with a Phillips PW3710, using the CuKα line, and Ni-filtered radiation (the wavelength was 1.54184 Å). The radiation was generated at 40 mA and 40 kV. Specimens were step-scanned as a random powder from 5° to 70°, 2θ range, and integrated over 2s per step.

The Environmental Scanning Electron Microscope (ESEM, Quanta200, FEI) was selected as the most suitable technique for the study of the morphology of the laterite-*meta*-halloysite-based materials with the advantage that the relative humidity can be controlled by both the water vapor pressure and the temperature in the ESEM-chamber. This observation approach permits avoiding the influence of cracks from the drying process necessary when the high vacuum SEM is used.

3. Results and discussion

3.1. Visual aspects of geopolymer samples exposed at room temperature

The geopolymer samples made with only laterite conserved the original raw mineral colour, dark red, while those manufactured with the reactive additive (20, 30 and 50% of *meta*-halloysite) have seen their colour fading from dark red to light red. This colour variation is due to the replacement of calcined laterite by a more whitish silica and alumina-rich aluminosilicate mineral (*meta*-halloysite) that reduced the overall iron content responsible for the red colour (Fig. 2). The white deposit of Na-carbonate disappears with the addition of metahalloysite (MH) which is better visible by the naked eye. The white salt deposit is known as the efflorescence phenomenon and is due to carbonation of excess Na. This change is due to the enrichment in reactive phases of the solid precursor, which will react with the Na^+ ions and fix them in the geopolymer network. This is in agreement with Criado et al. [31] who observed that if the solid precursor has enough of reactive phase, and if the reaction is fast enough, sodium is integrated into the geopolymer network structure and the migration of sodium ions to the surface where they carbonate is avoided. Next to the increased reactivity, the increase of the amount of reactive Al to Na makes sure that even for the activators with a high Na content (SiO_2/Na_2O = 0.75), the ratio Na/Al becomes almost one, so less excess Na is present if *meta*-halloysite is added.

3.2. Setting time

The average setting time values including standard deviation (represented by an error bar) of laterite based geopolymers blended with

Table 3
Chemical composition of laterite-*meta*-halloysite based geopolymer composites.

Geopolymer samples	Si/Al	Si/Fe	Al/Fe	($SiO_2/Na_2O = 1.04$; $H_2O/Na_2O = 9.78$)	($SiO_2/Na_2O = 0.92$; $H_2O/Na_2O = 10.45$)	($SiO_2/Na_2O = 0.75$; $H_2O/Na_2O = 12.04$)
				Na/Al	Na/Al	Na/Al
100/0	1.17	1.35	0.55	0.85	1.04	1.20
80/20	1.48	1.54	0.65	0.80	0.95	1.14
70/30	1.67	1.85	0.76	0.79	0.88	1.06
50/50	1.92	2.16	1.11	0.75	0.85	1.02

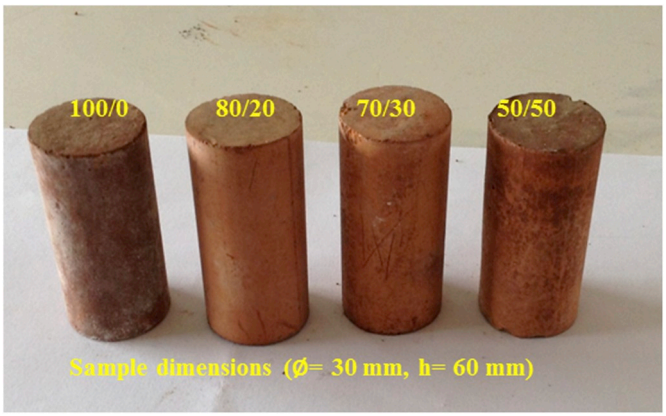

Fig. 2. Visual aspect of specimens exposed at room temperature for 360 days.

meta-halloysite (0, 20, 30 and 50 wt%) are represented in Fig. 3a–b, respectively. According to these Fig. (3a–3b), the initial and final setting times, decrease with an increase of MH600 content, and with the decreasing modulus of the activator. These two effects will be discussed separately. The reduction in setting time with addition of *meta*-halloysite clearly shows that *meta*-halloysite is more reactive than the calcined laterite, which contains metakaolinite as main reactive component. The amorphous *meta*-halloysite with a d_{50} of 8.40 μm is a finer powder than the calcined laterite with a d_{50} of 45.20 μm. A finer powder can in principle react faster, as the first step in the alkali activation is the dissolution of the powder by the alkaline solution. This reaction happens at the surface. However, care must be taken in this case as the specific surface area of the calcined laterite is larger than the one of *meta*-halloysite, in contradiction with what would be expected from the particle size distribution. A possible explanation is that the laterite contains some less or non-reactive material with a high specific surface area, while the reactive metakaolinite has a smaller specific surface area. The exact reason for this deviation could not be found. From a chemical point of view, there is an increase in reactive Al upon addition of *meta*-halloysite, e.g. the ratio Na/Al goes down. This extra Al from *meta*-halloysite is thus not just extra reactive material, but it also becomes quicker available in the reaction. This results in a faster build-up of the concentration of available Al-containing oligomers in solution. This accelerates the setting of the geopolymer pastes. The ratio Si/Al increases, however not all of this Si is reactive, as *meta*-halloysite also contains quartz.

The lower modulus of the activating solution, from 1.04 to 0.75 (Table 3), increase the reaction rate as expected. The activating solutions become more reactive thus faster breaking down the precursors. As such the concentration of building blocks in solution rises faster and the polycondensation will also start faster. Most of the Fe containing phases being stable, Fe probably only plays a minor role in the reaction. As such it will not be discussed here.

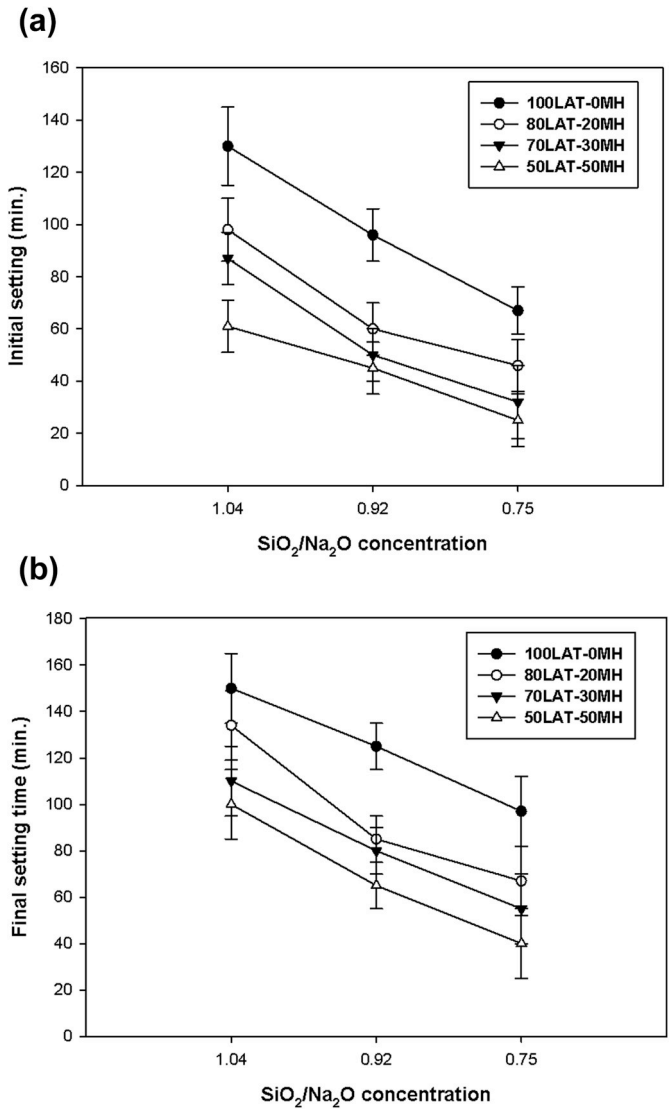

Fig. 3. Initial (a) and final (b) setting times of laterite-*meta*-halloysite based geopolymer. The setting time becomes shorter with increasing amount of *meta*-halloysite and Na/Al ratio.

3.3. Phase evolution

3.3.1. FTIR spectra analysis

The FTIR spectra of calcined laterite and *meta*-halloysite are plotted in Fig. 4a–b respectively. They are characterized by different vibrations belonging to Si–O, Si–O–Al, Al–O and Si–O–Si bonds namely Si–O–Si(Fe) stretching vibrations at 1006, 1034 and 1068 cm^{-1}, Si–O–Al vibration at 909 cm^{-1} and Si–O bending vibration at about 462, 369 cm^{-1}. The small sharp peaks at 3582-3657 cm^{-1} superimposed on the broad OH stretching band of water (Fig. 4b *meta*-halloysite) are related to the axial asymmetric and symmetric deformation modes of the hydroxyls

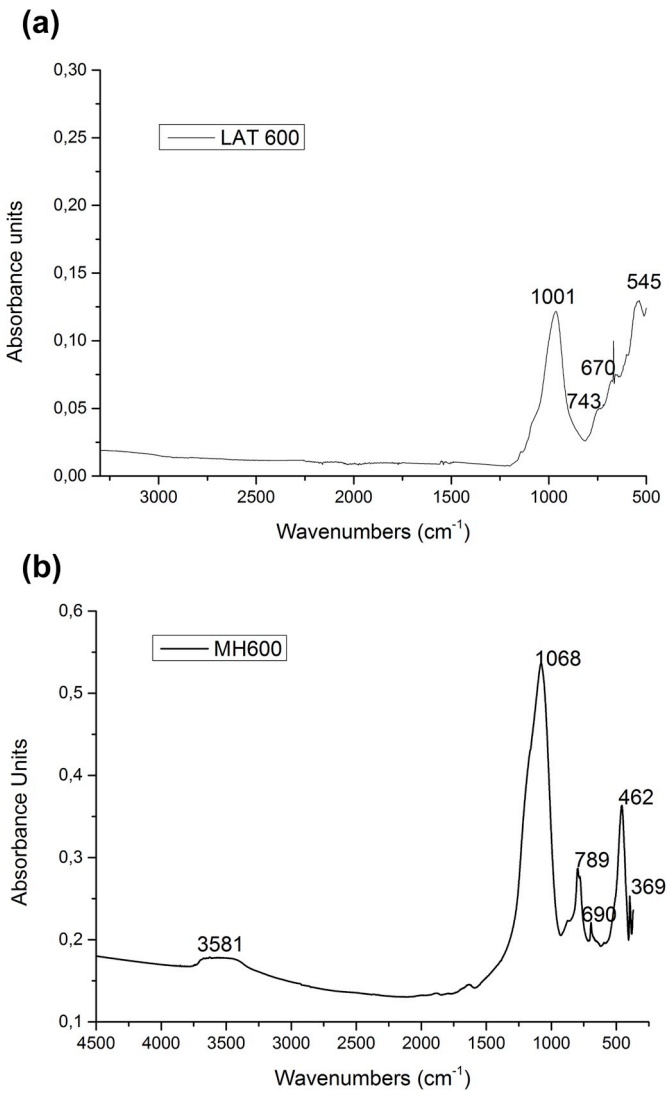

Fig. 4. FTIR spectra of calcined laterite (a) and *meta*-halloysite (b).

associated to Al atoms [30]. The presence of this absorption band indicates the non-complete transformation of halloysite to *meta*-halloysite during calcination. The bands at 743 and 790 cm^{-1} (Fig. 4a) and the ones at 789 and 690 cm^{-1} (Fig. 4b) were ascribed to the Si–O–Al bond symmetric stretching in metakaolin and *meta*-halloysite, respectively [32]. However, these sharp bands in *meta*-halloysite are also present in quartz which is present in the *meta*-halloysite sample.

The infrared spectra of geopolymer samples labeled 100/0, 80/20 and 50/50 are given in Fig. 5a, b and 5c. The broad band with maximum at 965–976 cm^{-1} in all geopolymer spectra (Fig. 5a–c) is due to Si–O–Si, Fe–O–Si and Si–O–Al vibrations of the growing geopolymeric network [33]. Compared to LAT600 and MH600, this band shifted from 1001 cm^{-1} respectively 1068 cm^{-1} to lower wavenumbers. It is remarkable that the peak positions in the final geopolymers are so close and independent of the amount of *meta*-halloysite used. It is an indication that finally, a comparable structure is formed but the amount of this reaction product may be different. The shift was expected and is due to the incorporation of tetrahedral Al in the silicate network [34]. The absorptions at 665–685 cm^{-1} are attributed to the Si–O–Al(IV) stretching of the tetrahedral network [35] but overlap with the band at 690 cm^{-1} from quartz. The bands at 389–432 cm^{-1} and 519–538 cm^{-1} are assigned to Si–O–Si (or Si–O–Al) symmetric stretching network and Fe–O stretching vibrations in tetrahedral and octahedral positions.

The remaining bands are less important ones. The band in the range

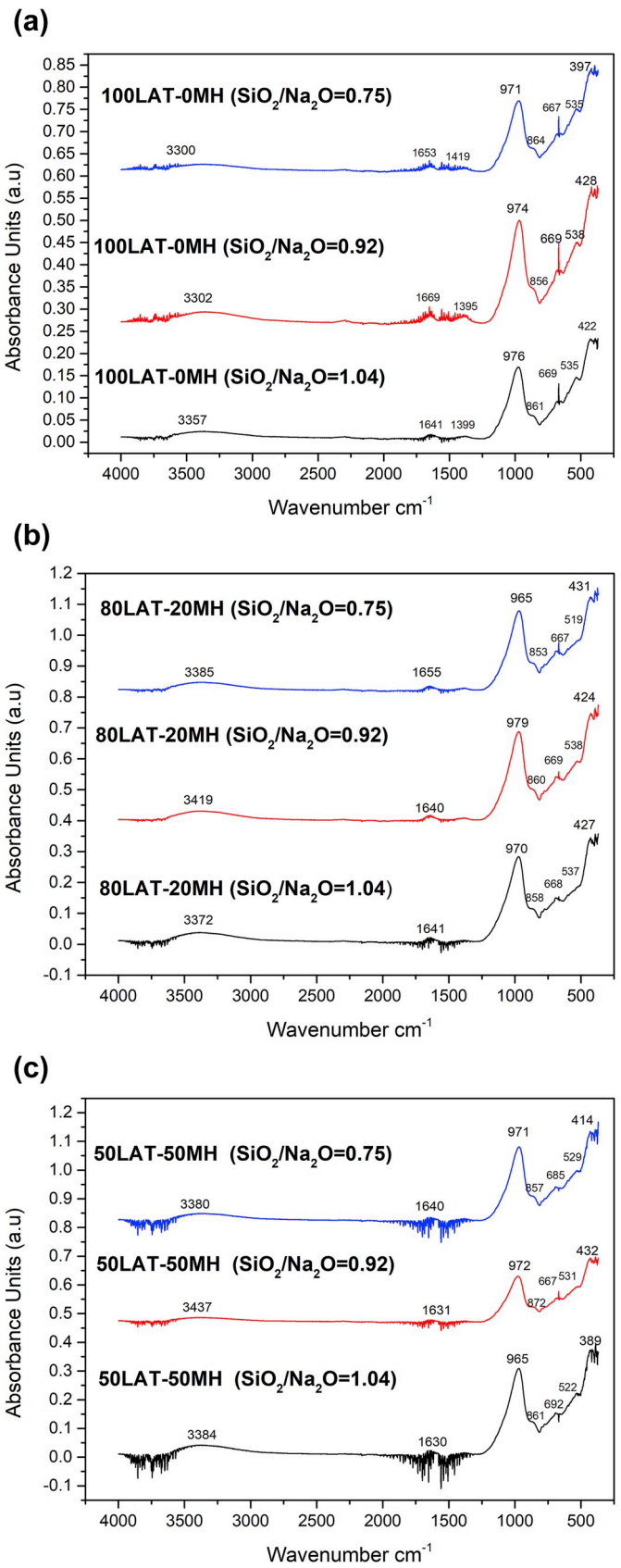

Fig. 5. FTIR spectra of laterite-based geopolymers blended with fine *meta*-halloysite labeled 100/0 (a), 80/20 (b) and 50/50 (c).

of 3300–3440 cm^{-1} is related to O–H stretching. The one situated in the interval between 1630 and 1670 cm^{-1} is attributed to H–O–H bending. The broad band located between 1399 and 1419 cm^{-1} in the samples labeled 100/0 (Fig. 5a) is due to the stretching of C–O in carbonates which is typical of Na_2CO_3 generated from the reaction of unreacted sodium ions and CO_2 from the atmosphere. This band is smaller in the FTIR spectra of 80/20 sample and almost invisible in the 50/50 specimens (Fig. 5b–c). It means that there is less carbonate formed, thus less efflorescence, as already observed on the surface of the samples. The shoulder at 858–872 cm^{-1} in the 100/0 geopolymer (Fig. 5a–b) can be assigned to the out-of-plane bending vibration of the carbonate ion [36–38]. However, this band is expected to be smaller and sharper than the one at about 1410 cm^{-1}, thus it overlaps with another one. The slight decrease in intensity of these bands with the addition of *meta*-halloysite from 0 to 50%, is due to the increase in reactive material (Tables 2 and 3). The *meta*-halloysite reacts with the alkaline solution and increases the amount of geopolymer network, thus also the amount of Na^+ needed to compensate for the Al in tetrahedral coordination. For the pure laterite the Na/Al ratio is 1.04 (10 M NaOH, $SiO_2/Na_2O = 0.75$) and it decreases to 0.84 for the 50/50 sample (see Table 3). It is well known that the stoichiometric ratio Na/Al is 1 [39], but the reaction slows down and the degree of reaction never reaches 100% [40]. Thus, the use of *meta*-halloysite also avoids the excess of alkali metal cations (Na^+) otherwise leading to the precipitation of carbonates on the surface, known as efflorescence. At present the role of Fe is still not well understood. It is however unlikely that the iron in Fe_2O_3 reacts but there might be a minor amount of reactive Fe^{2+} that gets incorporated into the network as Fe^{3+}, also needing Na^+ for charge compensation [41]. Reducing the amount of Na^+ used via the activator might be another way to get rid of the efflorescence but is not straightforward. The difficulty is that reducing the amount of total Na^+ in the activator also reduces the reactivity of the activator. The longer reaction time is mostly unwanted and leaves more time for carbonation. Reducing the amount of activator reduces the workability of the paste.

3.3.2. *X-ray diffraction analysis*

The X-ray patterns of laterite-based geopolymers blended with the fine powders of *meta*-halloysite (0, 20, 30 and 50%) are shown in Fig. 6a, b and 6c. It is observed that the presence of halo peaks (amorphous aluminosilicate phases) from 20 to 40° in 2 theta range increases with Si/Al and Na/Al molar ratios (see Table 3). This trend indicates that the partial substitution of calcined laterite by fine aluminosilicate (*meta*-halloysite) increased the amount of amorphous phase in the precursor which allows the formation of an extra glass or amorphous phase in the laterite-*meta*-halloysite based geopolymer matrix. The main phases like quartz (SiO_2, PDF# 46-1045); hematite (α-Fe_2O_3, PDF # 33-664); ilmenite ($FeTiO_3$, PDF# 29-733); maghemite (γ- Fe_2O_3, PDF# 15-615) and anatase (TiO_2, PDF# 4-447) present in the starting materials are still present after alkaline activation. There is no clear proof that these minerals have taken part in the geopolymerization reaction but these

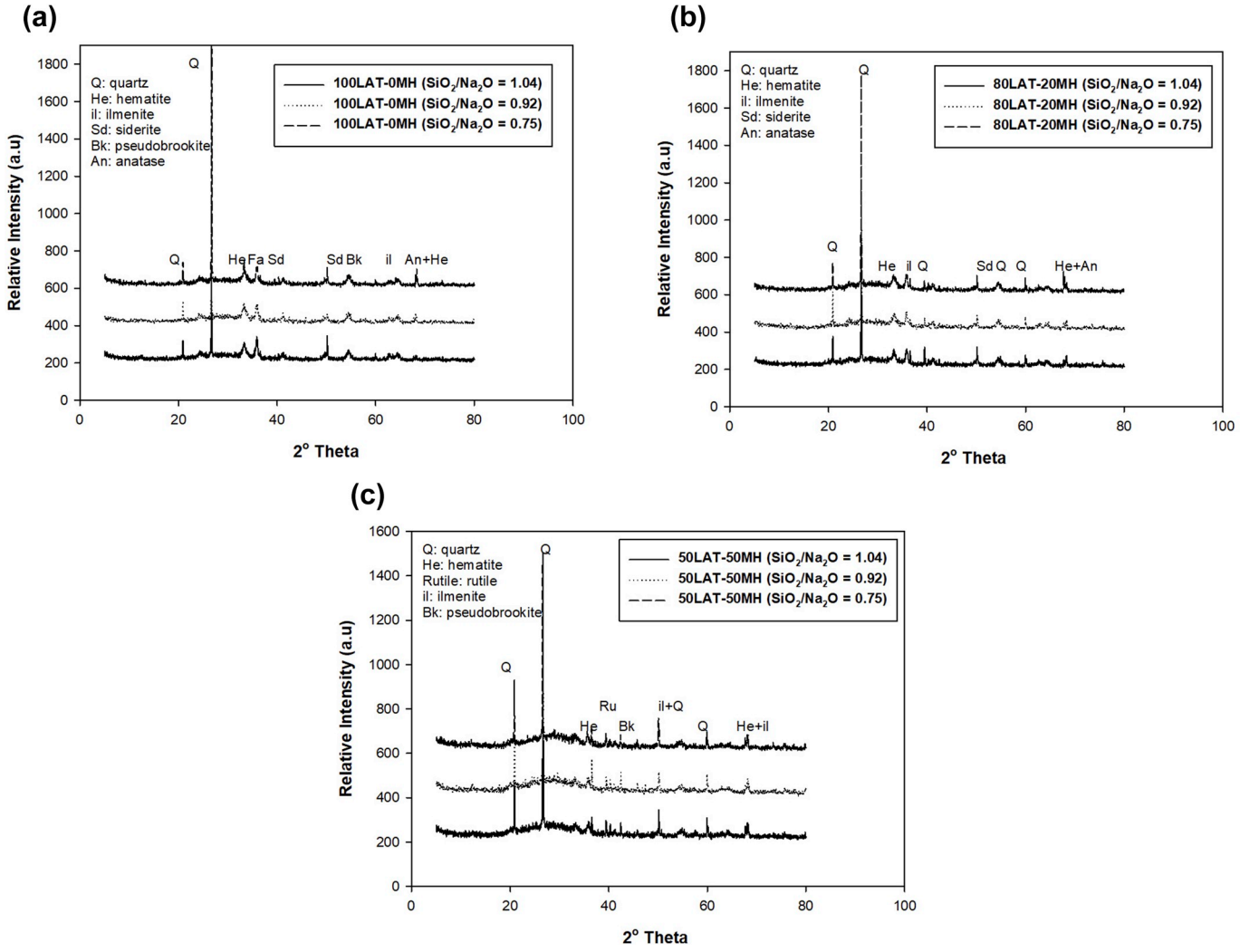

Fig. 6. XRD patterns of laterite-based geopolymers blended with fine *meta*-halloysite labeled 100/0 (a), 80/20 (b) and 50/50 (c).

phases act as inactive micro filler or micro-aggregate possibly improving the strength gained in the current study.

3.4. Mechanical strength

Fig. 7a–b highlight the data of the compressive strength testing conducted on the geopolymer samples labeled 100/0, 80/20, 70/30 and 50/50 cured at 7 and 28 days obtained under different alkaline solutions. The compressive strength almost doubles with 20% substitution and almost triples with 50% substitution (Table 3) with *meta*-halloysite. This increase does not seem to depend a lot on the Na/Al molar ratio. The increase is thus most spectacular with the addition of only 20% MH. The highest mechanical strength values are achieved on 50/50 samples with Si/Al (1.67 and 1.90) and Na/Al (1.02 and 1.06) ratios this is an activating solution with modulus $SiO_2/Na_2O = 0.75$. The higher compressive strength of the geopolymer binders containing extra reactive aluminosilicate (*meta*-halloysite) is due to two contributions: (i) the addition of the fine powder of reactive mineral provides additional reactive aluminosilicate species to build up the three-dimensional amorphous geopolymer structure giving the strength. (ii) The second contribution to strength is linked to the increase of the amount of Na^+ and OH^- available. The increase of the Na/Al ratio is needed as the stoichiometric ratio of Na/Al is 1 for aluminosilicate geopolymers. No more Al can be included in the network than can be compensated by Na. The higher alkalinity (activating solutions with $SiO_2/Na_2O = 0.92$ and 0.75, respectively) increases the release rate of Al, Si and maybe Fe containing building blocks from the solid precursor, increasing their concentration in solution, resulting in a faster and higher degree of polycondensation, and in compact and dense matrices. According to Pacheco-Torgal et al. [42], the increase in alkaline concentration in the paste mix increases the degree of hydration reactions and reduces the pore volumes by improving the microstructural properties which is beneficial to the mechanical performance. The increased MH600 addition lowers the Na/Al ratio (in the activating solutions with high Na_2O concentration namely $SiO_2/Na_2O = 0.92$ and 0.75) from 1.04 to 0.85 and 1.20 to 1.02 (see Tables 2 and 3) due to the available content of Al-species from additive MH600. The substitution of indurated laterite by the fine amorphous powder of *meta*-halloysite allowed the increase of Si/Al ratios from 1.17 to 1.92 and has demonstrated a positive effect on the mechanical strength development of laterite-based geopolymers in the ranges of 7–33 MPa and 12–45 MPa, respectively at 7-and 28-days. This trend is in agreement with the microscopic images obtained from pieces of fully consolidated specimens at 28 days of curing. The use of the fine aluminosilciate reactive powder of *meta*-halloysite, as reactive additive in our formulations, also contributed to reduce the efflorescence phenomenon observed in specimens without additive. This phenomenon is known to be deleterious to the development of mechanical strength due to the instability of geopolymer matrices. The trend of compressive strength is in line with the setting times and microstructural evolution results, see further. The link with setting time was not expected, but this is due to the faster reacting MH600, which also contains a larger fraction of reactive material. It is this addition of extra reactive material that increases the strength.

3.5. Drying shrinkage

Fig. 8 highlights the drying shrinkage of *meta*-halloysite based geopolymers at 7, 14, 21 and 28 days. It can be seen in Fig. 6 that the drying shrinkage decreases with an amount of mineral additive (*meta*-halloysite). This is due to the increase in reactive phase by adding *meta*-halloysite which improves the chemical mineralogy of starting materials resulting in a higher degree of geopolymerization accompanied with low drying shrinkage. Lower shrinkage can also be explained by an improvement of the N-A-S-H network with increasing the additive, accompanied by a reduction in water by evaporation, responsible for the decrease in length with time. According to Temuujin et al. [43], the shrinkage is related to water chemically bond to the geopolymer network structure. If a geopolymerization reaction is uncompleted, the non-reacted sodium ions and water will diffuse out of matrices network producing size reduction. Thus, there is a direct correlation between dimensional stability and geopolymerization advancement.

3.6. Microstructure

Fig. 9 shows electron microscope images of samples labeled 100/0, 80/20 and 50/50 made after 28 days curing time. As observed in Fig. 9, the use of the fine powder of *meta*-halloysite tends to prevent microcracks, pores and voids that were present in laterite-based geopolymers without additive mineral. In sample labeled 50/50, where the Si/Al, Si/Fe and Na/Al molar ratios were 1.92, 2.16 and 1.02, respectively (Table 3), the amount of binder phase was sufficient to embed different phases and make the geopolymer matrix denser and compact (Fig. 9c) with smaller pores compared to that of 100/0 and 80/20 which appeared less homogeneous and exhibited some larger pores and cracks (Fig. 9a and b). These molar ratios (Na/Al, Si/Fe and Si/Al) are responsible for the development of strength gained by the laterite based

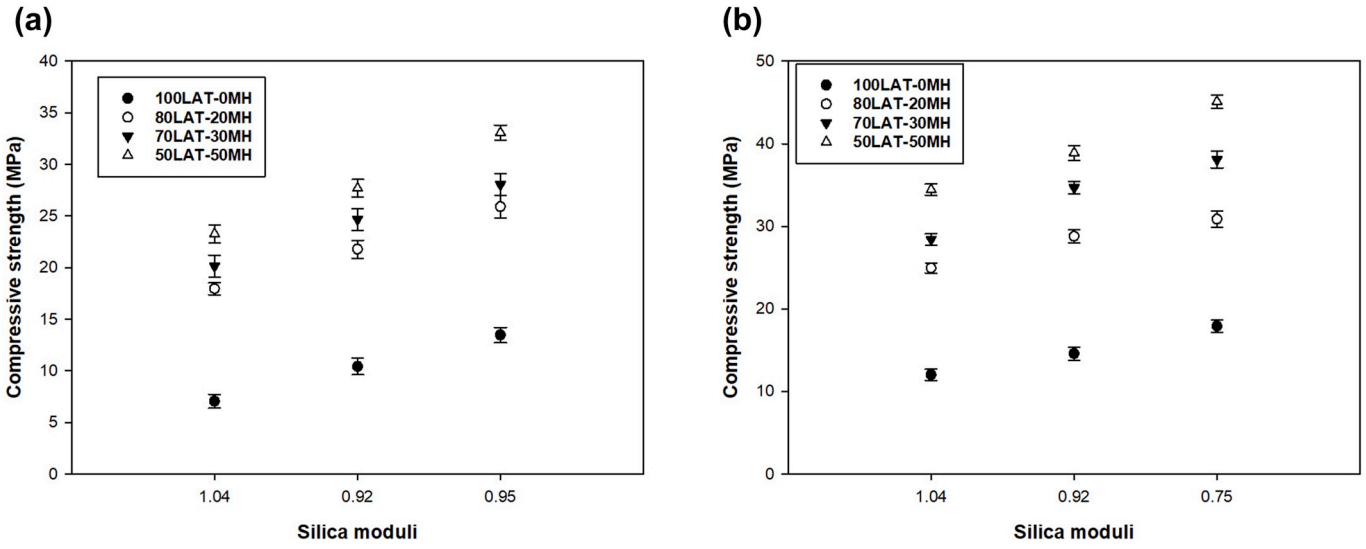

Fig. 7. Compressive strength of laterite-*meta*-halloysite based geopolymers cured at 7 (a) and 28 (b) days.

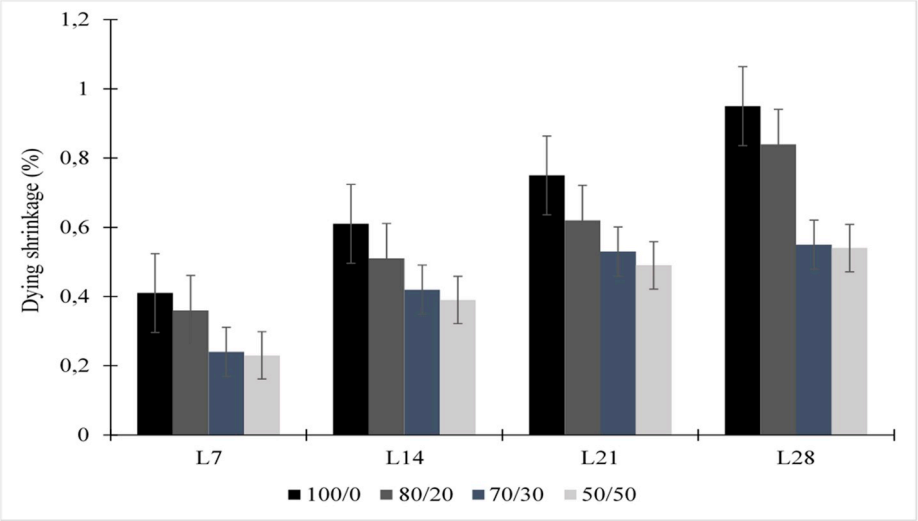

Fig. 8. Drying shrinkage of laterite-*meta*-halloysite based geopolymer cured at 28 days.

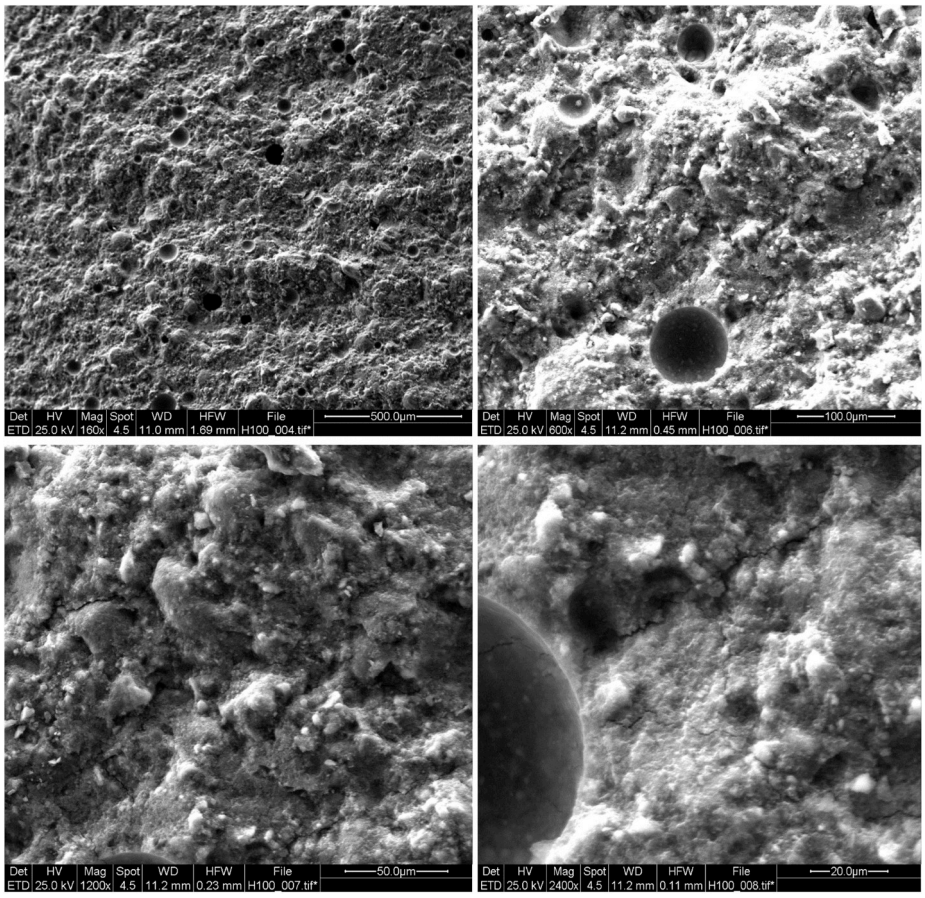

Fig. 9. Microscope images of 100/0 (a), 80/20 (b) and 50/50 (c) geopolymer mixtures.

geopolymer containing 50 wt% of *meta*-halloysite. However, the geopolymers (100/0 and 80/20 samples) characterized by Si/Al, Si/Fe and Al/Fe molar ratios of 1.17 (MPa) and 1.48 (MPa); 1.35 (MPa) and 1.54 (MPa); 0.55 (MPa) and 0.65 (MPa), respectively (Fig. 9a and b, Table 3), do not exhibit the same appearance in terms of the microstructure. This could be justified by the fact that, if more fine powder of reactive mineral is added, the reactive phase also increases. The changes in microstructure observed in SEM images are in line with the findings of other authors [32,33,44] who used a secondary aluminosilicate source as alumina, metakaolin, pumice and feldspars to improve the physico-chemical properties of geopolymer binder from volcanic scoria and metakaolin, respectively. They concluded that, with the more reactive additive mineral included into these systems, a higher dissolution extent of raw materials in alkaline media has been observed, the

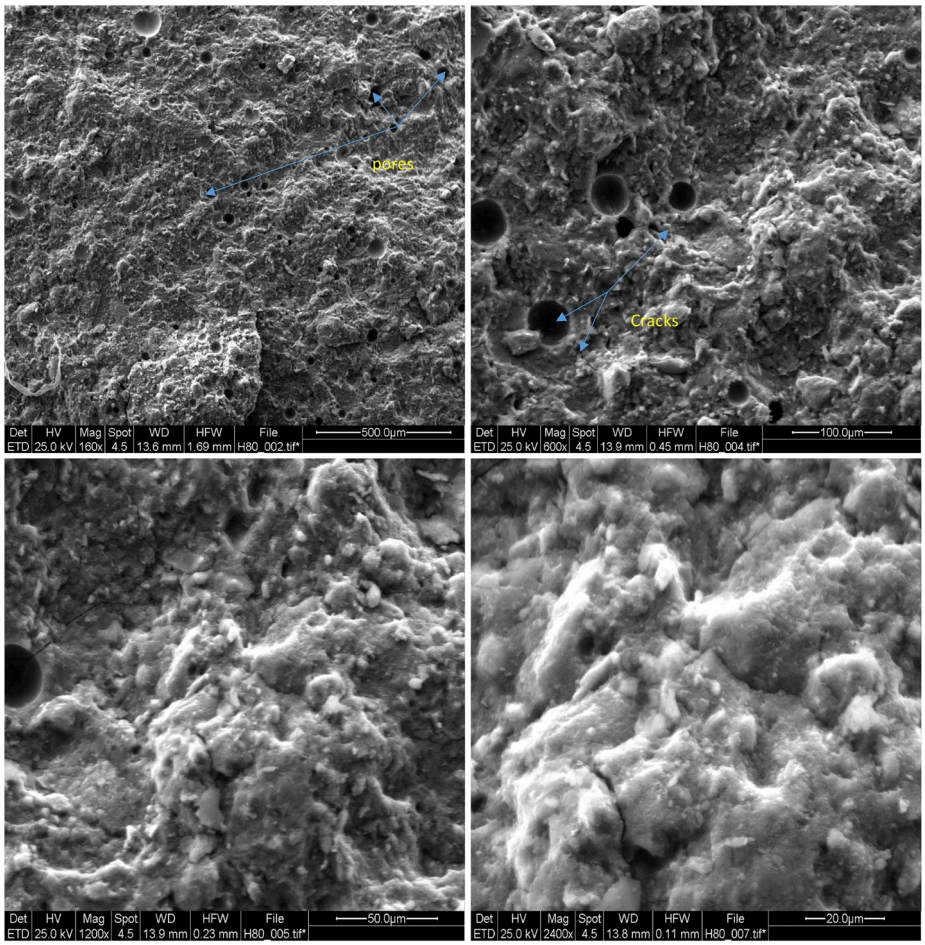

Fig. 9. (*continued*).

amorphous binder phase increased with Si/Al ratio in the range of 1–2, resulting in the development of higher strength. The highest strength obtained from higher alkalinity is probably due to the higher dissolution of reactive phase (aluminium and silicate species) which induced the better connectivity, cohesion and good binding between different particles into geopolymer matrices. In the case of samples without additive, the poor densification between different particles within the matrix can be related to the poor content of reactive phase and lower Si/Al (1.17) and Si/Fe (1.35) ratios. Then, with coarser particles mentioned earlier in paragraph 3.2, the calcined laterite cannot adopt the same behaviour in alkaline solution like *meta*-halloysite which is finer. This difference may be a good explanation for the appearance of coarser particles distributed within the geopolymer matrix of specimens labeled 100/0 and 80/20 (Fig. 9a and b). The coarse unreacted particles have also contributed to reinforce and densify the skeleton of geopolymer network by acting as reactive filler or micro-aggregates. Finally, the microstructure changes in geopolymer structure are linked to the trend of mechanical strength and setting times due larger fraction of binder resulting in good cohesion between different particles within the geopolymer network.

3.7. Water absorption

Table 4 displays the water absorption values of laterite based geopolymers with or without *meta*-halloysite as a secondary source of aluminosilicate. A decrease of roughly 50% is noticed with an increase in Si/Al, Si/Fe and Al/Fe molar ratios from 1.17 to 1.92, 1.35 to 2.16 and 0.55 to 1.11, respectively. The use of *meta*-halloysite increases the reactive phase favouring an extended polymerization of the aluminosilicate network to support the compressive loads, explaining the microstructures becoming less heterogeneous with Si/Al > 1.17. As a result, the samples of laterite geopolymer binders containing 20, 30 and 50 wt% MH absorb much less water. This is an indirect proof of a denser binder structure, with better developed silicate network and a lower porosity. Hence the increase in Na_2O concentration (corresponding to lower silicate modulus 0.92 and 0.75) induced the rise in hydroxyl ions which could favour the higher dissolution of solid precursor resulting in larger reactive quantities of stable products allowing the high polycondensation [45–47] resulting in compact structure with less pore formation justifying the decrease of water absorption values.

4. Conclusions

Calcined laterite at 600 °C can be used for geopolymerization but the resultant mechanical properties are weak. The addition of calcined halloysite, another clay mineral found in Cameroon and on many other places in the world can improve the mechanical properties of the material. Furthermore, upon the addition of 20, 30 and 50 wt% of fine *meta*-halloysite following conclusion can be drawn.

1. The initial and final setting times of fresh pastes decrease with increasing amounts of *meta*-halloysite and higher Na_2O concentration in the activating solution (lower SiO_2/Na_2O ratio). This promotes faster dissolution of the powder, followed by faster polycondensation, resulting in faster setting;
2. The highest compressive strength was obtained for geopolymer samples containing 50% of *meta*-halloysite and reached 33 and 45 MPa at 7- and 28-days, respectively. This improvement in strength is linked to the addition of *meta*-halloysite to the calcined

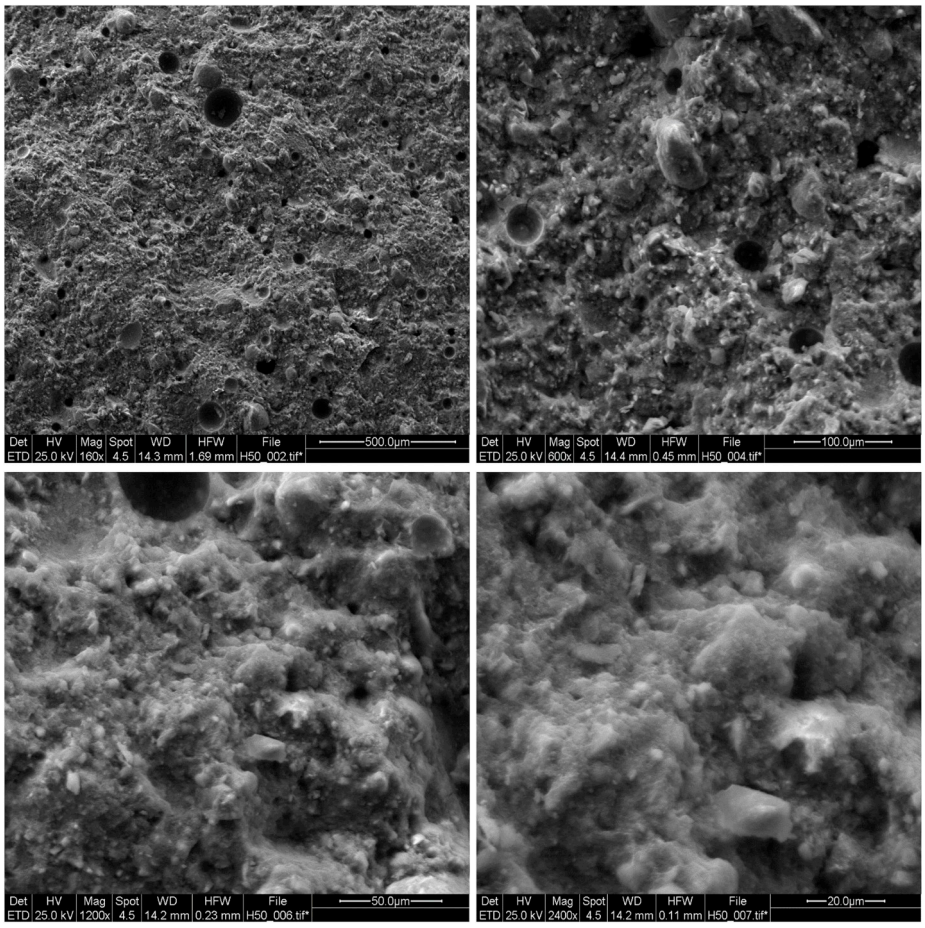

Fig. 9. (*continued*).

Table 4
Water absorption of geopolymer samples cured at 28 days carried out according to ASTM C642-06.

Geopolymer samples	Water absorption at 7 days	Standard deviation	Water absorption at 28 days	Standard deviation
100/0	14.17	0.35	10.55	0.32
80/20	11.48	0.44	8.65	0.40
70/30	9.67	0.25	7.76	0.29
50/50	7.92	0.16	4.11	0.25

laterite which increased the amount of amorphous SiO_2 and Al_2O_3 content in the system and, therefore, favored the dissolution of alumina and silica species. The decrease of water absorption and disappearance of efflorescence phenomenon accompanied this reticulation process;

3. Combining the alkali activation of calcined laterite with the addition of fine *meta*-halloysite, allowed the formation of geopolymer with dense and compact structure. From a morphological point of view, the homogeneity becomes higher when a high amount (50%wt) of *meta*-halloysite is present;
4. At a higher substitution level, a lower water absorption is observed due to a geopolymer that is closer to the stoichiometric ratio (Na/Al close to one). A more compact structure with less pores and crack formation was also observed under these circumstances;

Regarding the mechanical performances obtained in this study, the combined laterite with *meta*-halloysite in the range of 20, 30 and 50%wt made from the resulting geopolymers good candidate materials for future applications in civil engineering where higher strengths are required.

Acknowledgments

The authors are grateful to Dr. Mirko Braga and Dr. Pasquale Pansini, from R.S.A. Laboratory, from Ingessil S.r.l., Verona, Italy, for providing the alkaline solutions used in this work. This project also received the contribution of the Academic of Science for the Third World TWAS through the funding 15-079 RG/CHE/AF/AC_I to Dr. Elie Kamseu.

Appendix A. Supplementary data

Supplementary data to this article can be found online at https://doi.org/10.1016/j.matchemphys.2019.122268.

References

[1] Joseph Davidovits, Geopolymer Chemistry and Applications, fourth ed., 2015.
[2] a. Fernández-Jiménez, M. Monzó, M. Vicent, A. Barba, A. Palomo, Alkaline activation of metakaolin-fly ash mixtures: obtain of zeoceramics and zeocements, Microporous Mesoporous Mater. 108 (1–3) (2008) 41–49, https://doi.org/10.1016/j.micromeso.2007.03.024.
[3] John L. Provis, Rachel M. Harrex, Susan a Bernal, Duxson Peter, S J Van Deventer Jannie, Dilatometry of geopolymers as a means of selecting desirable fly ash sources, J. Non-Cryst. Solids 358 (16) (2012) 1930–1937, https://doi.org/10.1016/j.jnoncrysol.2012.06.001.
[4] E. Kamseu, A. Rizzuti, C. Leonelli, D. Perera, Enhanced thermal stability in K2O-Metakaolin-Based geopolymer concretes by Al2O3 and SiO2 fillers Addition.2010, J. Mater. Sci. 45 (2010) 1715–1724, https://doi.org/10.1007/s10853-009-4108-1.
[5] H.K. Tchakoute, A. Elimbi, E. Yanne, C.N. Djangang, Utilization of volcanic ashes for the production of geopolymers cured at ambient temperature, Cement Concr. Compos. 38 (2013) 75–81, https://doi.org/10.1016/j.cemconcomp.2013.03.010.

[6] Lecomte-Nana Gisèle, Hervé Goure-Doubi, Agnès Smith, Alain Wattiaux, Gilles Lecomte, Effect of iron phase on the strengthening of lateritic-based "geomimetic" materials, Appl. Clay Sci. 70 (2012) 14–21.

[7] Patrick N. Lemougna, U F Chinje Melo, Marie-Paule Delplancke, Hubert Rahier, Influence of the chemical and mineralogical composition on the reactivity of volcanic ashes during alkali activation, Ceram. Int. 40 (1) (2014) 811–820, https://doi.org/10.1016/j.ceramint.2013.06.072.

[8] H. Goure-Doubi, G. Lecomte-Nana, F. Nait-Abbou, B. Nait-Ali, A. Smith, V. Coudert, L. Konan, Understanding the strengthening of a lateritic ''geomimetic'' material, Constr. Build. Mater. 55 (2014) 333–340.

[9] Magdalena Lassinantti, Marcello Romagnoli, Simone Pollastri, Alessandro F. Gualtieri, Cement and concrete research inorganic polymers from laterite using activation with phosphoric acid and alkaline sodium silicate solution: mechanical and microstructural properties, Cement Concr. Res. 67 (2015) 259–270.

[10] R.C. Kaze, L.M. Beleuk, M.L. Fonkwe Djouka, A. Nana, E. Kamseu, U F Chinje Melo, C. Leonelli, The corrosion of kaolinite by iron minerals and the effects on geopolymerization, Appl. Clay Sci. 138 (2017) 48–62.

[11] Laurent Mbumbia, Albert Mertens, De Wilmars, Jacques Tirlocq, Performance characteristics of lateritic soil bricks fired at low temperatures: a case study of Cameroon, Constr. Build. Mater. 14 (2000) 121–131.

[12] Patrick N. Lemougna, Uphie F Chinje Melo, Elie Kamseu, Arlin B. Tchamba, Laterite based stabilized products for sustainable building applications in tropical countries: review and prospects for the case of Cameroon, Sustainability 3 (1) (2011) 293–305, https://doi.org/10.3390/su3010293.

[13] Kaze Cyriaque Rodrigue, Jean Noel Yankwa Djobo, Achile Nana, Herve Kouamo, Elie Kamseu Tchakoute, Uphie Chinje Melo, Cristina Leonelli, Hubert Rahier, Effect of silicate modulus on the setting, mechanical strength and microstructure of iron-rich aluminosilicate (laterite) based-geopolymer cured at room temperature, Ceram. Int. 44 (2018) 21442–21450, 2018.

[14] G.L. Lecomte-nana, E. Lesueur, J.P. Bonnet, G. Lecomte, Characterization of a lateritic geomaterial and its elaboration through a chemical route. 2009, Constr. Build. Mater. 23 (2) (2009) 1126–1132, https://doi.org/10.1016/j.conbuildmat.2008.06.009. Elsevier Ltd.

[15] Elie Kamseu, A. Nzeukou, P. Lemougna, Ndigui Billong, U.C. Melo, C. Leonelli, Induration of laterites in the tropical areas. Assessment for potential structural applications, Interceram 62 (6) (2013) 430–437.

[16] Esther A. Obonyo, Elie Kamseu, Patrick N. Lemougna, Arlin B. Tchamba, Uphie C. Melo, Cristina Leonelli, A sustainable approach for the geopolymerization of natural iron-rich aluminosilicate materials, Sustainability 6 (9) (2014) 5535–5553, https://doi.org/10.3390/su6095535.

[17] Nima Latifi, Eisazadeh Amin, Aminaton Marto, Strength behavior and microstructural characteristics of tropical laterite soil treated with sodium silicate-based liquid stabilizer, Environ. Earth Sci. (2014) 91–98, 2014.

[18] Patrick N. Lemougna, Kai-tuo Wanga, Qing Tang, E. Kamseu, N. Billong, U. Chinje Melo, Xue-min Cui, Effect of slag and calcium carbonate addition on the development of geopolymer from indurated laterite, Appl. Clay Sci. 148 (2017) 109–117.

[19] Rodrigue Cyriaque Kaze, Lynn Myllyam Beleuk à Moungam, Maria Cannio, Roberto Rosa, Elie Kamseu, Uphie Chinje Melo, Cristina Leonelli, Microstructure and engineering properties of Fe_2O_3(FeO)-Al_2O_3-SiO_2 based geopolymer composites, J. Clean. Prod. 199 (2018) 849–859, 2018.

[20] J. Zapała-Sławeta, The effect of meta-halloysite on alkali–aggregate reaction in concrete, J. Mater. Struct. 50 (2017) 217, https://doi.org/10.1617/s11527-017-1084-9.

[21] Z. Zhang, H. Wanga, X. Yao, Y. Zhu, Effects of halloysite in kaolin on the formation and properties of geopolymers, Cement Concr. Compos. 34 (2012) 709–715.

[22] Anupam Joshi, Carlos Montes, Saeid Salehi, Erez Allouche, Yuri Lvov, Optimization of geopolymer properties by coating of fly-ash microparticles with nanoclays, J. Inorg. Organomet. Polym. 25 (2015) 282–292, https://doi.org/10.1007/s10904-014-0105-1.

[23] G.W. Brindley, K. Robinson, D.M.C. MacEwan, The clay minerals halloysite and meta-halloysite, Nature 157 (1946) 225–226.

[24] D.M.C. Mac Ewan, The nomenclature of the halloysite minerals, Mineral. Mag. 28 (1947) 36–44, https://doi.org/10.1180/minmag.1947.028.196.08.

[25] K.J.D. MacKenzie, D.R.M. Brew, R.A. Fletcher, R. Vagana, Formation of aluminosilicate geopolymers from 1:1 layer-lattice minerals pre-treated by various methods: a comparative study, J. Mater. Sci. 42 (2007) 4667–4674.

[26] Hayami Takeda, Shinobu Hashimoto, Hiroaki Yokoyama, Sawao Honda, Yuji Iwamoto, Characterization of zeolite in zeolite-geopolymer hybrid bulk materials derived from kaolinitic clays, Materials 6 (2013) 1767–1778, https://doi.org/10.3390/ma6051767.

[27] G.-T. Joo, T.-K. Lee, M. Park, Y. Hwang, Compressive strength of geopolymers while varying the raw materials, J. Korean Chem. Soc. 49 (6) (2012) 575–580.

[28] Waijarean Naprarath, Asavapisit Suwimol, Kwannate Sombatsompop, Strength and microstructure of water treatment residue-based geopolymers containing heavy metals, Constr. Build. Mater. 50 (2014) 486–491.

[29] Bauluz Lázaro, Halloysite and kaolinite: two clay minerals with geological and technological importance, Rev. Real Acad. Ciencias Zaragoza. 70 (2015) 7–38. ISSN: 0370-3207.

[30] Kaze Cyriaque Rodrigue, Herve Kouamo, Theophile Tchakoute, Tchakouteu Mbakop, Jacques Richard Mache, Elie Kamseu, Uphie Chinje Melo, Cristina Leonelli, Hubert Rahier, Synthesis and properties of inorganic polymers (geopolymers) derived from Cameroon-meta-halloysite, Ceram. Int. 44 (2018) 18499–18508.

[31] M. Criado, A. Palomo, A. Fernandez-Jimenez, Alkali activation of fly ashes. Part I. Effect of curing condition on the carbonation of reaction products, Fuel 84 (2005), 2084-2054.

[32] Z. Yunsheng, S. Wei, L. Zongjin, Composition design and microstructural characterization of calcined kaolin-based geopolymer cement, Appl. Clay Sci. 47 (2010), 271– 27.

[33] Silviana Onisei, Alexios P. Douvalis, Annelies Malfliet, Arne Peys, Yiannis Pontikes, Inorganic polymers made of fayalite slag: on the microstructure and behavior of Fe, J. Am. Ceram. Soc. (2018) 1–13.

[34] H. Rahier, W. Simons, VanMele, M. Biesemans, Low-temperature synthesized aluminosilicate glasses .3. Influence of the composition of the silicate solution on production, structure and properties, J. Mater. Sci. 32 (1997) 2237.

[35] H.K. Tchakoute, C.H. Rüscher, J.N.Y. Djobo, B.B.D. Kenne, D. Njopwouo, Influence of gibbsite and quartz in kaolin on the properties of metakaolin-based geopolymer cements, Appl. Clay Sci. 107 (2015) 188–194.

[36] Gerald Fine, Edward Stolper, Dissolved carbon dioxide in basaltic glasses: concentrations and speciation, Earth Planet. Sci. Lett. 76 (1986) 263–278.

[37] A. Nazari, A. Bagheri, S. Riahi, Properties of geopolymer with seeded fly ash and rice husk bark ash, Mater. Sci. Eng. A 528 (2011) 7395–7401.

[38] Djobo Jean Noel Yankwa, Herve Kouamo Tchakoute, Navid Ranjbar, Elimbi Antoine, Leonel Noumbissie Tchadjie, Daniel Njopwouo, Gel composition and strength properties of alkali-activated oyster shell-volcanic ash: effect of synthesis conditions, J. Am. Ceram. Soc. (2016) 1–8, https://doi.org/10.1111/jace.14332.

[39] Hubert Rahier, Bruno Van Mele, Monique Biesemans, Wastiels Jan, Xiao Wu, Low-temperature reaction stoichiometry and structure of a model compound, J. Mater. Sci. 31 (1996) p80.

[40] Z. Zhang, H. Wang, J.L. Provis, X. Yao, F. Bullen, Y. Zhu, Quantitative kinetic and structural analysis of geopolymers. Part 1. The activation of metakaolin with sodium hydroxide, Thermochim. Acta 539 (2012) 23–33.

[41] Arne Peys, Claire E. White, Daniel Olds, Hubert Rahier, Bart Blanpain, Yiannis Pontikes, Molecular Structure of CaO-FeOx-SiO2 Resultant Inorganic Polymer Binders, 2018.

[42] F. Pacheco-Torgal, Z. Abdollahnejad, A.F. Camões, M. Jamshidi, Y. Ding, Durability of alkali-activated binders: a clear advantage over Portland cement or an unproven issue? Constr. Build. Mater. 30 (2012) 400–405.

[43] J. Temuujin, A. van Riessen, Effect of fly ash preliminary calcination on the properties of geopolymer, J. Hazard Mater. 164 (2009) 634–639.

[44] Elie Kamseu, Chiara Ponzoni, Chayanee Tippayasam, Taurino Rosa, Duangrudee Chaysuwan, Maria Chiara, Luisa Barbieri, Cristina Leonelli, Influence of fine aggregates on the microstructure, porosity and chemico-mechanical stability of inorganic polymer concretes, Constr. Build. Mater. 96 (2015) 473–483, https://doi.org/10.1016/j.conbuildmat.2015.08.090.

[45] A. Fernández-Jiménez, F. Puertas, Effect of activator mix on the hydration and strength behaviour of alkali-activated slag cements, Adv. Cem. Res. 15 (3) (2003) 129–136.

[46] Mandeep Kaur, Jaspal Singh, Manpreet Kaur, Synthesis of fly ash based geopolymer mortar considering different concentrations and combinations of alkaline activator solution, Ceram. Int. (2017), https://doi.org/10.1016/j.ceramint.2017.10.071.

[47] Jian He, Jie Yuxin, Jianhong Zhang, Yuzhen Yu, Guoping Zhang, Synthesis and characterization of red mud and rice husk ash-based geopolymer composites, Cement Concr. Compos. 37 (2013) 108–118.